Chen et al. *EPJ Quantum Technology* (2022) 9:10
https://doi.org/10.1140/epjqt/s40507-022-00128-z

EPJ Quantum Technology
a SpringerOpen Journal

RESEARCH Open Access

Storage and retrieval of microwave pulse in a crystal of molecular magnets based on four-wave-mixing

Jing Chen[1], Na Liu[1*], Chuanjia Shan[1], Hong Li[1] and Jibing Liu[1]

*Correspondence:
liuna@hbnu.edu.cn
[1]College of Physics and Electronic Science, Hubei Normal University, Huangshi, China

Abstract

In this paper, we consider a crystal of molecular magnets interacting with four alternating magnetic fields. When a DC magnetic field applies to molecular magnets, the energy levels of molecular magnets can be recognized as a four-level system. We consider four wave mixing process in the crystal of molecular magnets, By solving the Schrödinger equation, the analytic solutions of the probe and mixing magnetic fields are obtained. We have also numerically investigated the dynamical evolution of the probe and mixing magnetic fields. The results show that probe and mixing filed periodically oscillate in the crystal of molecular magnets medium. By adjusting the frequency detuning and the intensity of the coupled magnetic fields, the storage and retrieval of microwave field can be achieved in molecular magnets. In the end, the second-order correlation function is calculated and the anti-bunching effect can be achieved in this magnetic medium.

Keywords: Microwave; Molecular magnets; Storage and retrieval

1 Introduction

In recent years, the optical quantum storage has become an important focus of research activity [1–10]. Due to the importance of quantum optical memory, there are more and more researchers focusing on quantum storage. Based on balanced two-channel electromagnetically induced transparency, Zhu *et al.* [1] achieve a quantum memory for single-photon polarization qubits in laser-cooled rubidium atoms and the fidelity is higher than 99%. In particular, the efficiency of storing and retrieving of single-photon temporal waveforms can be reached as 90.6% in the single-channel quantum memory. By using time-reversal method, Phillips *et al.* [10] have shown that a light pulse can be trapped and stored in an optically thick medium and the maximum efficiency of storing and retrieving of optical pulses is obtained.

Besides, the nano-scale molecular magnets has aroused great interest because of its quantum magnetic properties [11–21]. Petukhov *et al.* [13] have studied the spin dynamics of molecular magnets in time-resolved magnetization experiments. They found that the phonon bottleneck with 10–100 ms characteristic relaxation time which had a great

influence on the magnetization kinetics of molecular magnets. Misiorny *et al.* [15] have proposed a magnetic switch process implementation scheme based on molecular magnets spin inversion. With the latest advances in nanotechnology, the transmission characteristics of molecular magnets have been studied experimentally and theoretically. The oscillation and wave propagation in noninteracting molecular magnet systems have been studied extensively [22–26]. When molecular magnets is subject to a DC magnetic field, the energy level of a single-molecule magnet split. By adjusting the parameters, we can obtain the corresponding energy level. The corresponding transition frequency is in the range of microwave. Take Fe_8 as an example, its transition frequency ω_{31} is about $10^{11}s^{-1}$ when H_0 = 14 koe. We propose a scheme to achieve storage and retrieval of microwave pulse in a crystal of molecular magnets. It is noted that molecular magnets have distinguished features, such as long spin decoherence time, low-density and sensitivity to external magnetic field, temperature, and so on. Takahashi *et al.* [27] measured the spin decoherence time $T_2 \sim 0.7$ microseconds for Fe_8 by high-frequency pulsed electron paramagnetic resonance. Takahashi *et al.* [28]also find that the decoherence time varies strongly as a function of temperature and magnetic field, and the optimal decoherence time rises to T_2 = 500 ms. So the spin decoherence time may be relevant to engineering molecular magnets for quantum information processing applications. It is important to achieve the storage of microwave photons in a single-molecule magnet because high-frequency waves support very high bandwidth. Besides, their high directionality reduces the possibility of eavesdropping, so our research may have potential applications in quantum communications. Shvetsov and coworkers [22] consider the electromagnetically induced transparency (EIT) in a crystal of molecular magnets which is driven by two (weak and strong) magnetic fields. The results show that EIT effect can be achieved in a crystal of molecular magnets and the imaginary part of the susceptibility is slightly effected by the distribution of longitudinal anisotropy constant D, whereas the effect of EIT is not suppressed. In the present study, we extend the former research on EIT [22] and four-wave mixing [29] to investigate the properties of quantum magnetic field in a crystal of molecular magnets. Firstly, we obtain the analytical solution for the probe and mixing quantum field. Secondly, we present an alternative scheme for achieving storage and retrieval of probe pulse in crystals of molecular magnets. The frequency of pulse is in range of microwave and the range of application is different from optical pulse in atomic medium. Thirdly, we give an alternative scheme for generating microwave pairs photons in crystals of molecular magnets and achieving the anti-bunching effect for microwave photons.

The paper is structured as follows. In Sec.II, we first describe the physical model and obtain the propagation equation of the probe and mixing magnetic field; then we obtain group velocities, absorption coefficient and relative phase by solving the dynamic evolution of the field equation. In Sec.III, we propose a scheme to achieve the storage and retrieval of microwave photons. In Sec.IV, we prepare a pair of photon and calculate the second-order correlation function between them. Eventually, we summarize the results of this work and give the conclusion in Sec. V.

2 Theoretical model and Hamiltonian

We consider a crystal of noninteracting molecular magnets which is subject to the DC magnetic field H_0. If z axis is the easy anisotropy axis of magnetic molecule and a DC magnetic field H_0 perpendicular to the z axis is applied to the crystal. Ten the Hamiltonian

of this system can be written as

$$\hat{H}_0 = -D\hat{S}_z^2 + \hat{H}_{\rm tr} - g\mu_B\hat{S}_x H_0, \tag{1}$$

where $\hat{H}_{\rm tr}$ is the transverse anisotropic energy operator. D is the longitudinal anisotropy constant, g is the Landé factor, and μ_B is the Bohr magneton. $\hat{S}_x$, $\hat{S}_y$, and $\hat{S}_z$ are the x, y, and z components of the spin operator. For Fe_8 molecules, the operator of the transverse anisotropy energy is $\hat{H}_{\rm tr} = K\hat{S}_y^2$, where K is the transverse anisotropy constant. The transverse anisotropy may be considered as a small perturbation relative to the longitudinal anisotropy, so we can ignore transverse anisotropy. Then the energy level of molecules without considering DC magnetic field can be written as

$$E_m = -Dm^2. \tag{2}$$

Due to the DC magnetic field, the molecule energy levels split. Using the method in [30], the expression of the energy level can be written as

$$E_m^{\pm} \simeq E_m \pm \frac{1}{2}\triangle E_m, \tag{3}$$

where $\triangle E_m$ is the splitting of the mth level. Its expression is

$$\triangle E_m \simeq \frac{2D(S+m)!}{[(2m-1)!]^2(S-m)!}\left(\frac{g\mu_B H_0}{2D}\right)^{2m}, \tag{4}$$

with S the molecule spin. We denote the eigenfunctions corresponding to E_m^- and E_m^+ by ψ_m^s and ψ_m^a, respectively. ψ_m^s (ψ_m^a) is a symmetric (antisymmetric) function with the expression

$$\psi_m^s = \frac{1}{\sqrt{2}}(\psi_m + \psi_{-m}), \tag{5a}$$

$$\psi_m^a = \frac{1}{\sqrt{2}}(\psi_m - \psi_{-m}), \tag{5b}$$

where $\psi_{\pm m}$ are eigenfunctions of the spin operator $\hat{S}_z$, which can be obtained from the eigen-equation $\hat{S}_z\psi_{\pm m} = \pm m\psi_{\pm m}$. For Fe_8 cluster, we obtain $S = 10$, $D = 0.31$ K, $g = 2$ and $K/D = 0.4$. We specify $\varepsilon_1 = E_{10}^-$, $\varepsilon_2 = E_{10}^+$, $\varepsilon_3 = E_9^-$ and $\varepsilon_4 = E_9^+$ with $\omega_{ef} = |\omega_e - \omega_f|/\hbar$ ($e \neq f = 1 \sim 4$) denoting the corresponding transition frequencies. For $H_0 = 14$ koe, we get $\omega_{21} = 0.58 \times 10^6 s^{-1}$, $\omega_{43} = 2.3 \times 10^8 s^{-1}$, $\omega_{31} = 8.1 \times 10^{11} s^{-1}$. The results show that the frequency of probe magnetic field is in the range of microwave. Next, we discuss the property of microwave field in this magnetic medium. As shown in Fig. 1, we can only consider the four lowest energy levels. The strong magnetic fields H_c (H_d) couple the state $|2\rangle$ to an excited state $|3\rangle$ ($|4\rangle$) with the frequency $\omega_c(\omega_d)$ while a quantum field $\hat{H'}_p$ drives the transition from the ground state $|1\rangle$ to an excited state $|3\rangle$ at the frequency ω_p. Then a mixing magnetic field $\hat{H'}_m$ appears at the frequency ω_m and couples the ground state $|1\rangle$ to an excited state $|4\rangle$ by a four-wave-mixing process. We assume that the propagation direction of four waves is along the z-axis, and H_c and $\hat{H'}_p$ polarizes along the y-axis, while H_d and $\hat{H'}_m$ polarizes along the x-axis as shown in Fig. 2. The magnetic field expression of two

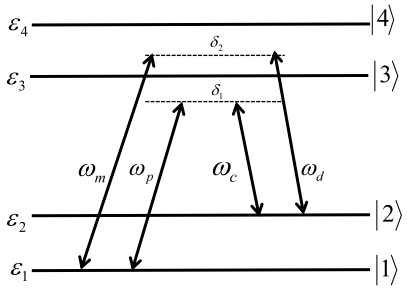

Figure 1 Schematic of energy level in a system of molecular magnets. Two strong magnetic fields H_c and H_d drive the transition from $|2\rangle$ to $|3\rangle, |4\rangle$, respectively. A quantum electromagnetic wave $\hat{H'}_p$ of frequency ω_p drives transition from $|1\rangle$ to $|3\rangle$, then a mixing field is generated with frequency ω_m. δ_1 and δ_2 are the single photon frequency detuning which are defined as $\delta_1 = \omega_{31} - \omega_p$, $\delta_2 = \omega_{41} - \omega_m$

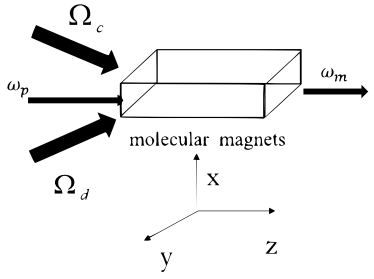

Figure 2 Sketch of the probe, mixing and control beam spatial configuration in a system of molecular magnets

strong magnetic fields are $(H_j/2)e^{-i\omega_j(t-z/c)+i\phi_j} + c.c.$ $(j = c, d)$ and the weak magnetic fields read $\hat{H'}_k = \int (\sqcap(\omega_k)\wp_{k1}/2)\hat{a}_k e^{i\omega_k z/c}\, d\omega_k$ $(k = m, p)$, where c is the speed of light in a vacuum and $\sqcap(\omega)$ a boxcar function, $\wp_{m1} = \sqrt{\frac{\hbar\omega_{14}}{2\varepsilon_0 V}}$ and $\wp_{p1} = \sqrt{\frac{\hbar\omega_{13}}{2\varepsilon_0 V}}$. $\hat{a}$ is the annihilation field operator, V is quantized volume and ε_0 is the dielectric constant. Under dipole approximation, the Hamiltonian of this system is [29, 31–33]

$$\hat{H} = \hat{H}_0 + \hat{H}_F + \hat{H}_L + \hat{H}_C, \tag{6a}$$

$$\hat{H}_F = \int \hbar\omega_m \hat{a}_m^\dagger \hat{a}_m \, d\omega_m + \int \hbar\omega_p \hat{a}_p^\dagger \hat{a}_p \, d\omega_p, \tag{6b}$$

$$\hat{H}_L = -\frac{g\mu_B}{2} \sum_j \hat{\vec{S}} \cdot \vec{H}_j e^{-i\omega_j(t-z/c)+i\phi_j} + H.c., \tag{6c}$$

$$\hat{H}_C = -\frac{g\mu_B}{2} \sum_k \hat{\vec{S}} \cdot \vec{\hat{H}}'_k + H.c., \tag{6d}$$

where the symbol $H.c.$ means the Hermitian conjugate, $\hat{H}_F$ represents two weak magnetic fields, $\hat{H}_L$ denotes the interaction between the magnetic molecule and two strong magnetic fields, while $\hat{H}_C$ represent the interaction between the magnetic molecule and two quantum fields. For simplicity, we assume the population of the system initially stay in the ground state. The state of the system has the general form [34]

$$|\psi(t)\rangle = |\psi_1(t)\rangle + |\psi_2(t)\rangle + |\psi_3(t)\rangle + |\psi_4(t)\rangle, \tag{7}$$

with

$$|\psi_1(t)\rangle = \int d\omega_p f_{\omega_p}(t)\hat{a}_p^\dagger |0\rangle_p |0\rangle_m |1\rangle$$

$$+\int d\omega_m f_{\omega_m}(t)\hat{a}_m^{\dagger}|0\rangle_p|0\rangle_m|1\rangle, \tag{8a}$$

$$|\psi_2(t)\rangle = \sum g(t)\hat{\sigma}_{21}|0\rangle_p|0\rangle_m|1\rangle, \tag{8b}$$

$$|\psi_3(t)\rangle = \sum b_1(t)\hat{\sigma}_{31}|0\rangle_p|0\rangle_m|1\rangle, \tag{8c}$$

$$|\psi_4(t)\rangle = \sum b_2(t)\hat{\sigma}_{41}|0\rangle_p|0\rangle_m|1\rangle. \tag{8d}$$

The notation $|n_1\rangle_p|n_2\rangle_m$ means the number of photons in modes ω_p and ω_m, $|n\rangle$ represent corresponding eigenstates of the molecule level. $b_1(t)$ and $b_2(t)$ stand for the probability amplitudes of the state $|3\rangle$ and $|4\rangle$, and $g(t)$ denotes the probability amplitude of state $|2\rangle$. $f_{\omega_p}(t)$ and $f_{\omega_m}(t)$ are the wave packet envelope functions of the probe and mixing magnetic fields, respectively. Those functions give a complete description of the state of this system [34]. In order to find their evolution, we insert the $\langle 0|_m\langle 1|_p\langle 1|$, $\langle 1|_m\langle 0|_p\langle 1|$, $\langle 0|_m\langle 0|_p\langle 2|$, $\langle 0|_m\langle 0|_p\langle 3|$, $\langle 0|_m\langle 0|_p\langle 4|$ into the Schrödinger equation and obtain

$$i\partial_t f_{\omega_p}(t) = \omega_p f_{\omega_p}(t) - \frac{1}{\hbar}Ng_p b_1(t)e^{-i\omega_p z/c}, \tag{9a}$$

$$i\partial_t f_{\omega_m}(t) = \omega_m f_{\omega_m}(t) - \frac{1}{\hbar}Ng_m b_2(t)e^{-i\omega_m z/c}, \tag{9b}$$

and

$$i\partial_t g(t) = \omega_2 g(t) - \left[\left(\Omega_c^0(z,t)\right)^* b_1(t) + \left(\Omega_d^0(z,t)\right)^* b_2(t)\right], \tag{10a}$$

$$i\partial_t b_1(t) = \omega_3 b_1(t) - g(t)\Omega_c^0(z,t) - \frac{g_p}{\hbar}\int d\omega_p f_{\omega_p}(t)e^{i\omega_p z/c}, \tag{10b}$$

$$i\partial_t b_2(t) = \omega_4 b_2(t) - g(t)\Omega_d^0(z,t) - \frac{g_m}{\hbar}\int d\omega_m f_{\omega_m}(t)e^{i\omega_m z/c}. \tag{10c}$$

We have defined $\Omega_c^0(z,t) = \Omega_c e^{-i\omega_c(t-z/c)+i\phi_c}$ and $\Omega_d^0(z,t) = \Omega_d e^{-i\omega_d(t-z/c)+i\phi_d}$. Ω_c and Ω_c are the Rabi frequencies of the strong magnetic fields which are defined as $\Omega_c = \frac{g\mu_B H_c}{2}\langle 3|\hat{S}_y|2\rangle$ and $\Omega_d = \frac{g\mu_B H_d}{2}\langle 4|\hat{S}_x|2\rangle$. If we set $\kappa_{12} = \frac{Ng_p^2}{\hbar^2 c}$, $\kappa_{14} = \frac{Ng_m^2}{\hbar^2 c}$, where N is the total number of molecules, g_p and g_m are the coupling constants which are defined as $g_p = \frac{g\mu_B \wp_{p1}}{2}\langle 3|\hat{S}_y|1\rangle$ and $g_m = \frac{g\mu_B \wp_{m1}}{2}\langle 4|\hat{S}_x|1\rangle$. After multiplying Eq. (9a)–(9b) by $e^{i\omega_p z/c}$, the quantum field amplitudes propagation equation can be obtained as

$$\left(\frac{1}{c}\partial_t + \partial_z\right)H_p(z,t) = i\kappa_{12}\beta_1(z,t), \tag{11a}$$

$$\left(\frac{1}{c}\partial_t + \partial_z\right)H_m(z,t) = i\kappa_{14}\beta_2(z,t), \tag{11b}$$

We have set $\beta_1(z,t) = b_1(t)e^{i\omega_p(t-\frac{z}{c})}$, $\beta_2(z,t) = b_2(t)e^{i\omega_m(t-\frac{z}{c})}$, $H_p e^{-i\omega_p(t-\frac{z}{c})} = \frac{g_p}{\hbar}\int d\omega_p f_{\omega_p}(t) \times e^{i\omega_p z/c}$ and $H_m e^{-i\omega_m(t-\frac{z}{c})} = \frac{g_m}{\hbar}\int d\omega_m f_{\omega_m}(t)e^{i\omega_m z/c}$ in Eq. (11a)–(11b). With these definitions, Eq. (10a)–(10c) read

$$\partial_t g(z,t) = i\left[e^{-i\phi_c}\Omega_c^*\beta_1(z,t) + e^{-i\phi_d}\Omega_d^*\beta_2(z,t)\right] - i\omega_2 g(z,t), \tag{12a}$$

$$\partial_t \beta_1(z,t) = i\triangle_1\beta_1(z,t) + iH_p(z,t) + ig(z,t)\Omega_c e^{i\phi_c}, \tag{12b}$$

$$\partial_t \beta_2(z,t) = i\Delta_2 \beta_2(z,t) + iH_m(z,t) + ig(z,t)\Omega_d e^{i\phi_d}, \tag{12c}$$

where $\Delta_1 = \delta_1 + i\frac{\gamma_1}{2}$ and $\Delta_2 = \delta_2 + i\frac{\gamma_2}{2}$, the γ_1 and γ_2 are the decay rate of level $|3\rangle$ and $|4\rangle$, respectively. Here all the energy differnces in Eq. (12a)–(12c) are taken relative to the energy of ground state $|1\rangle$. In order to obtain the solution of these equations, we first take the Fourier transform of Eq. (12a)–(12c) and obtain

$$\tilde{g}(z,\omega) = \frac{e^{-i\phi_c}\Omega_c^* \tilde{\beta}_1(z,\omega) + e^{-i\phi_d}\Omega_d^* \tilde{\beta}_2(z,\omega)}{\omega_2 - \omega}, \tag{13a}$$

$$\begin{aligned}\widetilde{\beta}_1(z,\omega) = {} & \kappa_{12}\frac{-|\Omega_d|^2 + (\omega-\omega_2)(\Delta_2+\omega)}{D(\omega)}\widetilde{H}_p(z,\omega) \\ & + \kappa_{12}\frac{e^{i\phi_{cd}}\Omega_c\Omega_d^*}{D(\omega)}\widetilde{H}_m(z,\omega),\end{aligned} \tag{13b}$$

$$\begin{aligned}\widetilde{\beta}_2(z,\omega) = {} & \kappa_{14}\frac{-|\Omega_c|^2 + (\omega-\omega_2)(\Delta_1+\omega)}{D(\omega)}\widetilde{H}_p(z,\omega) \\ & + \kappa_{14}\frac{e^{i\phi_{dc}}\Omega_d\Omega_c^*}{D(\omega)}\widetilde{H}_m(z,\omega),\end{aligned} \tag{13c}$$

where $\phi_{cd} = \phi_c - \phi_d$ is the phase difference between the coupling fields. $\tilde{g}(z,\omega)$, $\widetilde{H}_{p(m)}(z,\omega)$ and $\widetilde{\beta}_{1(2)}(z,\omega)$ are the Fourier transforms of $g(z,t)$, $H_{p(m)}(z,t)$ and $\beta_{1(2)}(z,t)$, respectively, and ω is the Fourier variable. We substitute Eq. (13a)–(13c) into Fourier-transformd Eq. (11a)–(11b) to obtain

$$\begin{aligned}&\partial_z \widetilde{H}_p(z,\omega) - \frac{i\omega}{c}\widetilde{H}_p(z,\omega) \\ &\quad = iK_1(\omega)\widetilde{H}_p(z,\omega) + iK_2(\omega)\widetilde{H}_m(z,\omega),\end{aligned} \tag{14a}$$

$$\begin{aligned}&\partial_z \widetilde{H}_m(z,\omega) - \frac{i\omega}{c}\widetilde{H}_m(z,\omega) \\ &\quad = iK_3(\omega)\widetilde{H}_m(z,\omega) + iK_4(\omega)\widetilde{H}_p(z,\omega),\end{aligned} \tag{14b}$$

with

$$K_1(\omega) = \kappa_{12}\frac{-|\Omega_d|^2 + (w-\omega_2)(\Delta_2+\omega)}{D(\omega)}, \tag{15a}$$

$$K_2(\omega) = \kappa_{12}\frac{e^{i\phi_{cd}}\Omega_c\Omega_d^*}{D(\omega)}, \tag{15b}$$

$$K_3(\omega) = \kappa_{14}\frac{-|\Omega_c|^2 + (w-\omega_2)(\Delta_1+\omega)}{D(\omega)}, \tag{15c}$$

$$K_4(\omega) = \kappa_{14}\frac{e^{i\phi_{dc}}\Omega_d\Omega_c^*}{D(\omega)}, \tag{15d}$$

where $D(\omega) = (\Delta_1+\omega)|\Omega_d|^2 + (\Delta_2+\omega)|\Omega_c|^2 - (\Delta_1+\omega)(\Delta_2+\omega)(\omega-\omega_2)$. The solution of Eq. (14a)–(14b) can be obtained as follows,

$$\widetilde{H}_p(z,\omega) = \left(R_1 e^{i\lambda_1(\omega)z}c + R_2 e^{i\lambda_2(\omega)z}\right)\widetilde{H}_p(0,\omega)$$

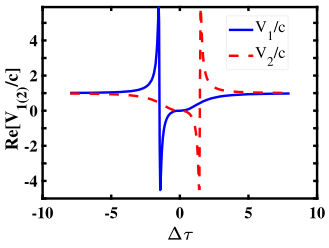

Figure 3 Group velocities Re[V_1/c] (blue solid line) and Re[V_2/c] (red dashed line) as function of the dimensionless photon detuning $\Delta\tau$ with $z_0 = 0.5$ mm, $\tau = 10\ \mu s$ $\gamma_1\tau = 50$, $\gamma_2\tau = 60$, $\kappa_{12}\tau z_0 = 2 \times 10^4$, $\kappa_{14}\tau z_0 = 3 \times 10^4$

$$+ R_3\left(e^{i\lambda_2(\omega)z} - e^{i\lambda_1(\omega)z}\right)\widetilde{H}_m(0,\omega), \tag{16a}$$

$$\widetilde{H}_m(z,\omega) = R_4\left(e^{i\lambda_2(\omega)z} - e^{i\lambda_1(\omega)z}\right)\widetilde{H}_p(0,\omega) + \left(R_1 e^{i\lambda_2(\omega)z} + R_2 e^{i\lambda_1(\omega)z}\right)\widetilde{H}_m(0,\omega), \tag{16b}$$

where $\widetilde{H}_p(0,w)$ and $\widetilde{H}_m(0,w)$ are the initial condition at the $z = 0$, and the expression of $\lambda_{1(2)}$ are defined as

$$\lambda_{1(2)}(\omega) = \frac{w}{c} + \frac{1}{2}\left(K_1(\omega) + K_3(\omega) \mp K_5(\omega)\right), \tag{17}$$

where the expression of $K_5(\omega)$, R_1, R_2, R_3 and R_4 are given in the Appendix. We only focus on the adiabatic regime, where $\lambda_{1(2)}$ can be extended to the fast convergence power series of dimensionless transformation variables, i.e., $\lambda_{1(2)} = (\lambda_{1(2)})_{w=0} + w/V_{1(2)} + \mathcal{O}(w^2)$, $\alpha_{1(2)} = (\lambda_{1(2)})_{w=0}$, $R_i = R_i(\omega)_{w=0} + \mathcal{O}(\omega)$ and $A_i = R_i(\omega)_{w=0}$ $(i = 1,2,3,4)$ [29, 32–37]. Hence, the inverse Fourier Transform of Eq. (16a)–(16b) is given by

$$H_p(z,t) = \left[(A_1 H_p(\eta_1) - A_3 H_m(\eta_1)\right]e^{i\alpha_1 z} + \left[(A_2 H_p(\eta_2) + A_3 H_m(\eta_2)\right]e^{i\alpha_2 z}, \tag{18a}$$

$$H_m(z,t) = \left[(A_2 H_m(\eta_1) - A_4 H_p(\eta_1)\right]e^{i\alpha_1 z} + \left[(A_4 H_p(\eta_2) + A_1 H_m(\eta_2)\right]e^{i\alpha_2 z}, \tag{18b}$$

where $\eta_{1(2)} = t - z/V_{1(2)}$, $\alpha_{1(2)} = \frac{1}{2}(K_1(0) + K_3(0) \mp K_5(0))$ and the group velocities of two modes are defined as

$$\frac{1}{V_{1(2)}} = \frac{1}{c} + \frac{1}{2}\left(K_{1m}(0) + K_{3m}(0) \mp K_{5m}(0)\right), \tag{19}$$

where $K_{1m}(0), K_{3m}(0)$ and $K_{5m}(0)$ are given in the Appendix. From equations (18a)–(18b), we obtain that the probe and mixing magnetic fields contain two propagation modes for the general frequency component, and the two modes of magnetic fields have independent group velocities. We plot the group velocity of probe and mixing magnetic field as a function of dimensionless $\Delta\tau$ which is the ratio of δ_1 to the $\tau_0(10^7 s^{-1})$ in Fig. 3. From Fig. 3, we see that one wave packet mode propagates with negative group velocity and another wave packet mode propagates with positive group velocity in the range of $-2 < \Delta\tau < 2$. We also obtain slow light when $\Delta\tau$ is small. Therefore, we can obtain two sets of speed-matched probe-mixing magnetic field pairs that reach the detector after time of delay. When the

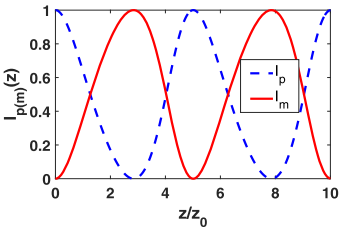

Figure 4 (**a**) Intensities of the microwave probe magnetic field pulse I_p (solid line) and mixing magnetic field pulse I_m (dashed line) as a function of z/z_0. We set $\phi_{cd} = \pi/4$, $H_p(t_c) = H_m(t_c)$ and $\Delta\tau = 40$, the other parameters are chosen as those used in the plot of Fig. 3

$\Delta\tau$ is small, the group velocities of the two propagation modes are equal. As a result, a pair of fields with matching group velocity can be obtained.

In what follows, we consider the group velocities $V_1 = V_2 = V$, i.e., $\eta_1 = \eta_2 = \eta$. We can then obtain the intensity of probe and mixing magnetic field. From Equations (18a)–(18b), the expressions for $|H_p(z,t)|^2$ and $|H_m(z,t)|^2$ can be given as

$$\begin{aligned}\left|H_p(z,t)\right|^2 &= |a|^2\left|H_p(\eta)\right|^2 + |b|^2\left|H_m(\eta)\right|^2 + ab^* H_p(\eta)H_m^*(\eta) \\ &\quad + a^* bH_p^*(\eta)H_m(\eta),\end{aligned} \tag{20a}$$

$$\begin{aligned}\left|H_m(z,t)\right|^2 &= |c|^2\left|H_p(\eta)\right|^2 + |d|^2\left|H_m(\eta)\right|^2 + cd^* H_p(\eta)H_m^*(\eta) \\ &\quad + c^* dH_p^*(\eta)H_m(\eta),\end{aligned} \tag{20b}$$

where the coefficient a, b, c and d are defined as

$$a = A_1 e^{i\alpha_1 z} + A_2 e^{i\alpha_2 z}, \tag{21a}$$

$$b = A_3\left(e^{i\alpha_2 z} - e^{i\alpha_1 z}\right), \tag{21b}$$

$$c = A_4\left(e^{i\alpha_2 z} - e^{i\alpha_1 z}\right), \tag{21c}$$

$$d = A_1 e^{i\alpha_2 z} + A_2 e^{i\alpha_1 z}. \tag{21d}$$

If we define the relative phase between probe and mixing magnetic fields as $\Phi = \mathrm{Arg}[H_p(z,t)H_m^*(z,t)]$, so we can find the relative phase from the following equation

$$\begin{aligned}H_p(z,t)H_m^*(z,t) &= ac^*\left|H_p(\eta)\right|^2 + bd^*\left|H_m(\eta)\right|^2 \\ &\quad + ad^* H_p(\eta)H_m^*(\eta) + c^* bH_p^*(\eta)H_m(\eta).\end{aligned} \tag{22}$$

Afterwards, by analyzing expressions in Eq. (20b)–(21a) and Eq. (22), we discuss different propagation of probe and mixing magnetic field by fixing the reference system at the peak of the weak photon pulse ($t_c = z/v$), Therefore, we only need to show the intensity of probe and mixing magnetic field changes in the space dimension z. The normalized intensity of probe and mixing magnetic fields are defined as

$$I_{p(m)}(z) = \frac{|H_{p(m)}(z,t_c)|^2}{|H_{p(m)}(z,t_c)|^2 + |H_{m(p)}(z,t_c)|^2}. \tag{23}$$

We plot the relative phase and intensity of probe and mixing magnetic field as a function of z/z_0 in Fig. 4 and Fig. 5. Figure 4 indicates that the intensity and the relative phase of

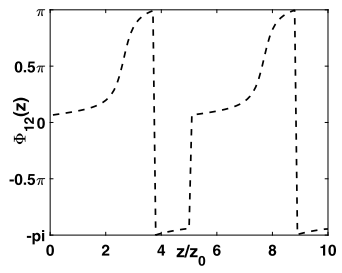

Figure 5 The relative phase Φ_{12} as a function of z/z_0, other parameters are chosen as those used in the plot of Fig. 4

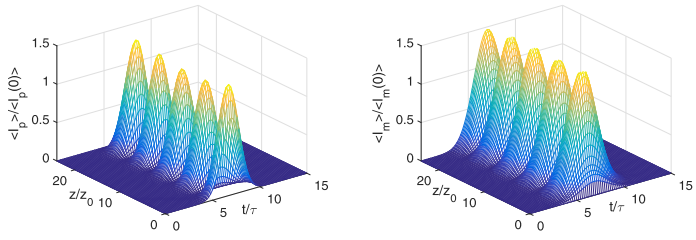

Figure 6 (**a**) Intensity of the microwave probe pulse as a function of position and time. (**b**) Intensity of the microwave FWM pulse as a function of position and time. These parameters are explained in the text

probe and mixing magnetic field periodically oscillate in the crystal of molecular magnets medium. This implies that one can recover probe field at the output of the medium by properly choosing the parameter. The relative phase between two modes is

$$\Phi_{12}(z) = \mathrm{Arg}\big[H_p(z,t_c)H_m^*(z,t_c)\big]. \tag{24}$$

3 Numerical simulations and analysis

In this section, we show the microwave probe pulse propagation by numerically integrating Eq. (13a)–(13c). Moreover, we also present the process of storage and retrieval of a microwave probe pulse. To simulate the pulse propagation in time and distance, we adopt Gaussian profiles of temporal width $\tau = 10\ \mu s$ centered at $t_c = 7.5\tau$. For the single-molecular-magnets medium, we select $z_0 = 0.5$ mm, $\gamma_1\tau = 50$, $\gamma_2\tau = 60$, $\kappa_{12}\tau z_0 = 2\times10^4$, $\kappa_{14}\tau z_0 = 3\times10^4$, $|\Omega_c|\tau = |\Omega_d|\tau = 1000$, $\delta_1 = 0$ and $\delta_2\tau = 1.5\times10^{-2}$, With these parameters, the intensity of the probe pulse and FWM pulse as a function of position and time is shown in Fig. 6. We can see that the intensity of microwave probe pulse and microwave FWM pulse exhibit complementary periodic oscillations in the process of propagation by the evolution equation of the numerical integrated system. Namely, we can obtain output photon with frequency of ω_m, when the input photon frequency is ω_p The behavior of the intensities of probe pulse and FWM pulse fits well with the theoretical model.

In order to achieve the storage and retrieval process, we use the control beams of form

$$\Omega_c(t)/\Omega_c(0) = 1 - \tanh\big[\sigma(t-t_1)\big] + \tanh\big[\sigma(t-t_2)\big], \tag{25}$$

with $\Omega_c(0)\tau = \Omega_d(0)\tau = 1000$, $\delta_1 = 0$, $\delta_2\tau = 1.5\times10^{-2}$, $\sigma = 1/\tau$, $t_1 = 11\tau$, $t_2 = 24\tau$, and other parameter are the same in the plot Fig. 3. We show an example of the microwave probe

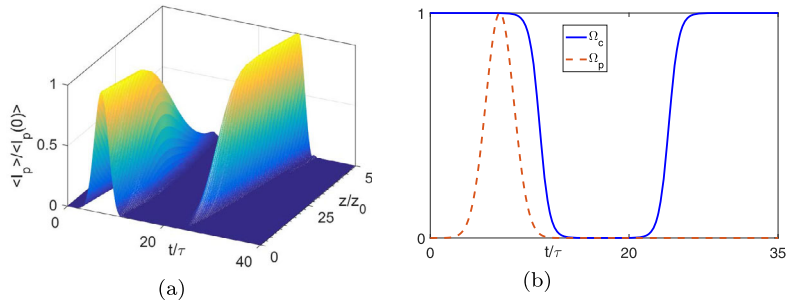

Figure 7 (**a**) Storage and retrieval of microwave probe pulse as a function of position and time. (**b**) Temporal profile of the coupling beams. These parameters are explained in the text

pulse can be recovered by appropriately choosing the control fields in Fig. 7(a), the storage time of the probe pulse is approximately given by $t_2 - t_1 = 13\tau$. Shown in Fig. 7(b) is the temporal profile of the control field(blue solid line) and initial microwave probe pulse(red dashed line) of the medium.

4 Generating paired photons and two-photon intensity correlation function

In this section, we consider when the injected quantum state is a single-photon wave packet of the specific form follows [38–41]

$$|1\rangle_{\varpi} = \int_{-\infty}^{\infty} d\omega' P_1(\varpi + \omega')\hat{a}^{\dagger}(\omega')|0\rangle, \tag{26}$$

Here, P_1 means amplitude and satisfies $\int_{-\infty}^{\infty} d\omega' |P_1|^2 = 1$, the ϖ is the central frequency of wave packet. We assume that only one photon with central frequency ω_p and no phonon with central frequency ω_m, Hence, the initial state for the system is

$$|\psi_{\text{in}}\rangle = |1\rangle_p |0\rangle_m \tag{27}$$

In general, at any given time, the state of a molecular magnet system can be written as

$$|\psi_{\text{out}}\rangle = \sum_{nm} \alpha_{nm}(t)|n\rangle_p |m\rangle_m. \tag{28}$$

Using the identity $\sum_{nm} |\alpha_{nm}(t)|^2 = 1$, we can work out the coefficients $\alpha_{nm}(t)$ according to the following equation:

$$\begin{aligned} &\langle\psi_{\text{out}}|F(\hat{H}_p^{\dagger}, \hat{H}_m, \hat{H}_p^{\dagger}\hat{H}_m, \ldots)|\psi_{\text{out}}\rangle \\ &\quad = \langle\psi_{\text{in}}|F(\hat{H}_p^{\dagger}, \hat{H}_m, \hat{H}_p^{\dagger}\hat{H}_m, \ldots)|\psi_{\text{in}}\rangle, \end{aligned} \tag{29}$$

where $\hat{H}_p$ and $\hat{H}_m$ denote the probe and mixing field operators and F denotes the combinations of products of the field operators. In the case of a small gain, there is one photon generated with the frequency ω_p when a single-probe photon is injected the crystal of molecular magnets. At the same time, a mixing photon is produced at the frequency ω_m by stimulated Raman process. We can write the final state of the system as

$$|\psi(t)\rangle = \alpha_{10}|1\rangle_p |0\rangle_m + \alpha_{20}|2\rangle_p |0\rangle_m + \alpha_{21}|2\rangle_p |1\rangle_m. \tag{30}$$

The physical meaning of each is clear. α_{10} indicates the probability with which the injected probe photon is in the ground state. α_{20} describes the photons generated by the excitation emission in the probe mode, but no mixing photon is produced. α_{20} is the probability amplitude of the photons produced by the stimulus in the probe mode and the photon generated in the mixing mode. The second term in the equation exists when the pumping field is very weak, which can excite the FWM process. When the pump field is strong enough, this term α_{20} will disappear from the equation. In this case, the state of the system is simplified to the following form

$$\left|\psi(t)\right\rangle = |\alpha_{10}1\rangle_p|0\rangle_m + |\alpha_{21}\|2\rangle_p|1\rangle_m. \tag{31}$$

With the help of Eq. (29), the expression of $|\alpha_{21}|^2$ and $|\alpha_{10}|^2$ can be obtained as

$$|\alpha_{21}|^2 = 2|c|^2P_1^2(\eta), \tag{32a}$$

$$|\alpha_{10}|^2 = \left(|a|^2 + |b|^2 - 4|c|^2\right)P_1^2(\eta), \tag{32b}$$

It is worth noting that for high gain media, higher order terms such as $\alpha_{32}|3\rangle_p|2\rangle_m$ will appear in Eq. (31), then we can obtain photon pairs with frequencies ω_p and ω_m by theoretical calculations. In order to show the time-dependent properties of the generated photon pairs, we work out the correlation function between the ω_p and ω_m with a time delay τ_d,

$$G^{(2)}_{H_1-H_2}(\tau_d) = \left\langle \hat{H}_1^\dagger(t)\hat{H}_2^\dagger(t+\tau_d)\hat{H}_2(t+\tau_d)\hat{H}_1(t)\right\rangle. \tag{33}$$

Using the Eq. (29), and the intensity correlation function $G^{(2)}_{H_1-H_2}(\tau_d)$ can be expressed as

$$\begin{aligned} G^{(2)}_{H_1-H_2}(\tau_d) = &\left(\int d\omega P_1^2(\omega)|a|^2 + \int d\omega|c|^2\right)\int d\omega|b|^2 \\ &+ \int d\omega P_1^2|b|^2 \int d\omega|c|^2 + \left|\int d\omega e^{i\omega\tau_d}a^*b\right|^2 \\ &+ \int d\omega e^{-i\omega\tau_d}P_1^2(\omega)a^*b\int d\omega e^{-i\omega\tau_d}cd^* \\ &+ \int d\omega e^{i\omega\tau_d}P_1^2(\omega)ab^*\int d\omega e^{i\omega\tau_d}c^*d. \end{aligned} \tag{34}$$

The second-order correlation function $g^{(2)}_{H_1-H_2}(\tau_d)$ is defined as $g^{(2)}_{H_1-H_2}(\tau_d) = G^{(2)}_{H_1-H_2}(\tau_d)/G^{(1)}_{H_1}(0)G^{(1)}_{H_2}(0)$. In order to discuss the quantum properties of probe and mixing magnetic fields, we also plot the second-order correlation function as a function of delay time τ_d in Fig. 8. The evolution of second-order correlation function is similar to that of the damped Rabi oscillations. The anti-bunching effect of weak magnetic field is achieved when $g^{(2)}_{H_1-H_2}(\tau_d) < 1$. When a photon of frequency ω_p is generated, then a photon of frequency ω_m is generated by four-wave mixing after a delay τ_d. Thus, a pair of photons of frequencies ω_p and ω_m is obtained in the crystal of molecular magnets system.

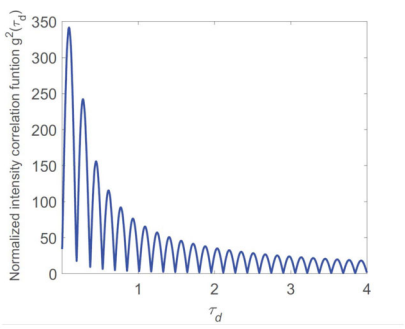

Figure 8 The second-order correlation function with the delay time τ_d. Other parameters are chosen as those used in the plot of Fig. 6

5 Conclusion

In this paper, we study the propagation dynamics of probe and mixing magnetic field in the crystal of molecular magnets. In the adibatic regime, we obtain the analytic solution for the probe and mixing magnetic field with two different modes. For suitable parameter range, the results show that two modes have similar group velocity and can retain the initial shape for propagating in the magnetic medium. The intensity and relative phase of probe and mixing magnetic field in the crystal of molecular magnets medium exhibit periodic oscillation in propagation. Also, we have demonstrated that, at certain positions in the magnetic medium, the microwave single photon superposition state can be stored and recovered by adjusting the intensity of coupling magnetic field. Finally, we calculate the second-order correlation function of probe photon and mixing photon, yielding microwave correlated photons pair and achieving the anti-bunching effect for microwave photons in the crystal of molecular magnets.

Appendix

Here we give expression of relevant terms in Eqs. (16a)–(16b), (17) and (19) in the main article:

$$R_1(\omega) = \frac{K_3(\omega) - K_1(\omega) + iK_5(\omega)}{2iK_5(\omega)},$$

$$R_2(\omega) = \frac{K_1(\omega) - K_3(\omega) + iK_5(\omega)}{2iK_5(\omega)},$$

$$R_3(\omega) = \frac{K_2(\omega)}{iK_5(\omega)},$$

$$R_4(\omega) = \frac{K_4(\omega)}{iK_5(\omega)},$$

$$K_5(\omega) = \sqrt{\left[K_1(\omega) - K_3(\omega)\right]^2 + 4K_2(\omega)K_4(\omega)}$$

and

$$D_m(0) = |\Omega_d|^2 + |\Omega_c|^2 + \Delta_1\omega_2 + \Delta_2\omega_2 - \Delta_1\Delta_2,$$

$$K_{1m}(0) = \kappa_{12}\frac{(|\Omega_d|^2 - \Delta_2 + \omega_2)D_m(0) + (\Delta_2 - \omega_2)D(0)}{D^2(0)},$$

$$K_{2m}(0) = -\kappa_{12}\frac{e^{i\phi_{cd}}\Omega_c\Omega_d^* D_m(0)}{D^2(0)},$$

$$K_{3m}(0) = \kappa_{14}\frac{(|\Omega_c|^2 - \Delta_1 + \omega_2)D_m(0) + (\Delta_1 - \omega_2)D(0)}{D^2(0)},$$

$$K_{4m}(0) = -\kappa_{14}\frac{e^{i\phi_{dc}}\Omega_d\Omega_c^* D_m(0)}{D^2(0)},$$

$$K_{5m}(0) = \frac{(K_1(0) - K_3(0))(K_{1m}(0) - K_{3m}(0))}{\sqrt{K_5(0)}} + \frac{2K_{2m}(0)K_4(0) + 2K_2(0)K_{4m}(0)}{\sqrt{K_5(0)}}.$$

Acknowledgements
We first thank Dr. Chen Li for revising the English of this article. This project is supported by the Program for Innovative Teams of Outstanding Young and Middle-aged Researchers in the Higher Education Institutions of Hubei Province (Grant No. T2020014), and in part by the program of Outstanding Innovation Team of Hubei Normal University (No: T201902).

Funding
This work is supported by HBNU.

Abbreviations
EIT, electromagnetically induced transparency; DC, direct-current.

Availability of data and materials
The data sets supporting the results of this article are included within the article.

Declarations

Ethics approval and consent to participate
Not applicable.

Consent for publication
Not applicable.

Competing interests
The authors declare that they have no competing interests.

Authors' contributions
JC, JL together conceived the idea for the study. JC and NL performed the numerical calculation and plotted the figures. All the authors discussed and got the conclusion of the manuscript. HL and JL wrote the manuscript. All authors reviewed the manuscript. All authors read and approved the final manuscript.

Publisher's Note

Received: 18 August 2021 Accepted: 16 March 2022 Published online: 08 April 2022

References

1. Wang Y, Li J, Zhang S, Su K, Zhou Y, Liao K, Du S, Yan H, Zhu S-L. Efficient quantum memory for single-photon polarization qubits. Nat Photonics. 2019;13(5):346.
2. Thomas SE, Hird TM, Munns JHD, Brecht B, Saunders DJ, Nunn J, Walmsley IA, Ledingham PM. Raman quantum memory with built-in suppression of four-wave-mixing noise. Phys Rev A. 2019;100:033801.
3. Simon C, Afzelius M, Appel J, de La Giroday AB, Dewhurst S, Gisin N, Hu C, Jelezko F, Kröll S, Müller J et al. Quantum memories. Eur Phys J D. 2010;58(1):1–22.
4. Lvovsky AI, Sanders BC, Tittel W. Optical quantum memory. Nat Photonics. 2009;3(12):706.
5. Hedges MP, Longdell JJ, Li Y, Sellars MJ. Efficient quantum memory for light. Nature. 2010;465(7301):1052.
6. Raczynski A, Zaremba J, Zielinska-Kaniasty S. Electromagnetically induced transparency and storing of a pair of pulses of light. Phys Rev A. 2004;69(4):043801.
7. Nunn J. Towards high-speed optical quantum memories. Nat Photonics. 2010;4(4):218–21.
8. Yang C, Bai Z, Huang G. Ultraslow optical solitons and their storage and retrieval in an ultracold ladder-type atomic system. Phys Rev A. 2014;89(2):351.
9. Jiang KJ, Deng L, Payne MG. Ultraslow propagation of an optical pulse in a three-state active Raman gain medium. Phys Rev A. 2006;74(4):520.
10. Phillips DF, Fleischhauer A, Mair A, Walsworth RL, Lukin MD. Storage of light in atomic vapor. Phys Rev Lett. 2001;86(5):783.

11. Chudnovsky EM. Quantum hysteresis in molecular magnets. Science. 1996;274(5289):938–9.
12. Garanin DA, Chudnovsky EM. Quantum entanglement of a tunneling spin with mechanical modes of a torsional resonator. Phys Rev X. 2011;1(1):011005.
13. Misiorny M, Barnas J. Spin polarized transport through a single-molecule magnet: current-induced magnetic switching. Phys Rev B. 2007;76(5):054448.
14. Liu J, Liu N, Liu T, Shan C, Li H, Zheng A, Xie X-T. Microwave induced phase grating in molecular magnets via cross phase modulation. J Magn Magn Mater. 2020;503:166609.
15. Lancaster T, Moeller JS, Blundell SJ, Pratt FL, Baker PJ, Guidi T, Timco GA, Winpenny RE. Observation of a level crossing in a molecular nanomagnet using implanted muons. J Phys Condens Matter. 2011;23(24):242201.
16. Chudnovsky EM, Tejada J. Macroscopic quantum tunneling of the magnetic moment. 1st ed. Cambridge: Cambridge University Press; 1998. https://doi.org/10.1017/CBO9780511524219.
17. Liu J, Liu N, Shan C, Liu T, Li H, Zheng A, Xie X-T. Electromagnetically induced grating in a crystal of molecular magnets system. Phys Lett A. 2016;380(31–32):2458–64.
18. Calero C, Chudnovsky E, Garanin D. Magneto-elastic waves in crystals of magnetic molecules. Phys Rev B. 2007;76(9):094419.
19. Lü X-Y, Song P-J, Liu J-B, Yang X. N-qubit w state of spatially separated single molecule magnets. Opt Express. 2009;17(16):14298–311.
20. Liu J-B, Xie X-T, Wu Y. Acoustic solitary wave and breather in molecular magnets via electromagnetically induced transparency. Europhys Lett. 2010;89(1):17006.
21. Liu J-B, Lü X-Y, Liu N, Wang M, Liu T-K. Microwave solitons in molecular magnets via electromagnetically induced transparency. Phys Lett A. 2009;373(4):413–7.
22. Shvetsov AV, Vugalter GA, Grebeneva AI. Theoretical investigation of electromagnetically induced transparency in a crystal of molecular magnets. Phys Rev B, Condens Matter. 2006;74(5):54416.
23. Timm C, Elste F. Spin amplification, reading, and writing in transport through anisotropic magnetic molecules. Phys Rev B. 2006;73(23):235304.
24. Tokman ID, Vugalter GA. Nonstationary behavior of a high-spin molecule in a bifrequency alternating current magnetic field. Phys Rev A. 2002;66(1):144.
25. Tokman ID, Vugalter GA, Grebeneva AI, Pozdnyakova VI. Nonstationary interaction of a high-spin molecule or a rare Earth metal ion with an acoustic wave and an alternating current magnetic field. Phys Rev B. 2003;68(17):174426.
26. Tokman ID, Shvetsov AV. The interrelation between the Faraday effect and the inverse Faraday effect in a magnetic medium and the terahertz inverse Faraday effect in single molecule magnets. Eur Phys J B. 2009;72(1):97–104.
27. Takahashi S, Tol JV, Beedle CC, Hendrickson DN, Sherwin MS. Coherent manipulation and decoherence of $s = 10$ single-molecule magnets. Phys Rev Lett. 2009;102(8):087603.
28. Takahashi S, Tupitsyn IS, van Tol J, Beedle CC, Hendrickson DN, Stamp PCE. Decoherence in crystals of quantum molecular magnets. Nature. 2011;476(7358):76–9.
29. Wu Y, Yang X. Four-wave mixing in molecular magnets via electromagnetically induced transparency. Phys Rev B. 2007;76(5):054425.
30. Garanin DA. Spin tunnelling: a perturbative approach. J Phys A, Math Gen. 1991;24(2):61.
31. Lü X-Y, Liu J-B, Tian Y, Song P-J, Zhan Z-M. Single molecular magnets as a source of continuous-variable entanglement. Europhys Lett. 2008;82(6):64003.
32. Wu Y, Yang X. Giant Kerr nonlinearities and solitons in a crystal of molecular magnets. Appl Phys Lett. 2007;91(9):36.
33. Xie X-T, Li W, Li J, Yang W-X, Yuan A, Yang X. Transverse acoustic wave in molecular magnets via electromagnetically induced transparency. Phys Rev B. 2007;75(18):184423.
34. Viscor D, Ahufinger V, Mompart J, Zavatta A, Rocca GCL, Artoni M. Two-color quantum memory in double-Λ media. Phys Rev A. 2012;86(5):053827.
35. Wu Y, Yang X. Electromagnetically induced transparency in *v*-, Λ-, and cascade-type schemes beyond steady-state analysis. Phys Rev A. 2005;71:053806.
36. Wu Y, Saldana J, Zhu Y. Large enhancement of four-wave mixing by suppression of photon absorption from electromagnetically induced transparency. Phys Rev A. 2003;67:013811.
37. Wu Y, Yang X. Highly efficient four-wave mixing in double-λ system in ultraslow propagation regime. Phys Rev A. 2004;70:053818.
38. Wu Y, Payne MG, Hagley EW, Deng L. Preparation of multiparty entangled states using pairwise perfectly efficient single-probe photon four-wave mixing. Phys Rev A. 2004;69(6):063803.
39. Yuan C-H, Lu C-P, Zhang W, Deng L. Generating correlated (2 + 1)-photon pairs in an active-Raman-gain medium. Phys Rev A. 2009;79(3):033804.
40. Deng L, Payne MG, Huang G, Hagley EW. Formation and propagation of matched and coupled ultraslow optical soliton pairs in a four-level double- system. Phys Rev E. 2005;72(2):055601.
41. Raymer M, Noh J, Banaszek K, Walmsley I. Pure-state single-photon wave-packet generation by parametric down-conversion in a distributed microcavity. Phys Rev A. 2005;72(2):023825.